SIMULATION OF TURBULENT FLOW IN A SUDDEN CONTRACTION WITH A POROUS INSERT

Reinaldo M. Orselli[1]
Marcelo J.S. De-Lemos[2]
Departamento de Energia - IEME
Instituto Tecnológico de Aeronáutica - ITA
12228-900 - São José dos Campos - SP, Brazil
[1]orselli@mec.ita.br
[2]delemos@ita.br

Abstract. *The purpose of this work is to investigate numerically the influence of a porous insert on an incompressible turbulent flow in a pipe that suffers a sudden contraction. The Reynolds number is 93,600 based on the pipe outlet diameter. The flow equations are discretized by using the control volume method and the SIMPLE algorithm is applied for the velocity-pressure coupling. In all cases, the macroscopic k-ε Low-Reynolds turbulence model will be employed. For an initial numerical validation, a simulation is carried out without the porous insert in order to be compared with an experimental result. Afterwards, the porous insert will be considered in the numerical calculations, parameters such as permeability and thickness are varied in order to analyze their effects on the flow pattern. Also, the flow losses obtained with the porous insert are calculated and compared with that obtained from the calculations without the porous insert.*

Keywords: *sudden contraction, porous media, turbulent flow, numerical solution.*

1. Introduction

There are several applications in the industry and science which involves flow with porous insertions, such as, engineering systems in oil extraction, filters, flow through forests, crops and cooling in electrical equipments. Concerning the flow through a sudden contraction, its direction is changed abruptly and so a recirculation is observed just after the contraction that is called *vena contracta*, which, in turn, can be defined as the section where the effective flow is minimum (S_c).

Flow studies in pipes with sudden contraction have been the subject of numerous publications. Streeter (1961) showed experimental values of minor losses as a function of S_2 / S_1 for turbulent flows. Astarita & Greco (1968) reported some measurements of the pressure on the wall in the laminar flow range and also discussed the literature already published in this subject. Durst & Loy (1985) investigated laminar flows for S_2 / S_1 = 0.285. In that work experimental and numerical results for velocity profiles, *vena contracta* dimensions and pressure losses were compared.

Many articles have recently been published in the literature where a numerical simulation was performed, using linear and non-linear *k-ε* macroscopic turbulence models, in a turbulent flow past a sudden expansion, Assato & de Lemos (2000, 2002, 2003), Assato et. al. (2005), or contraction, Assato & de Lemos (2004a-d), of a planar channel partially filled with a porous insert. Generally, the articles showed a comparison of results simulated with both linear and non-linear turbulence models and parameters such as porosity, permeability, thickness of the porous insert were varied in order to analyze their effects on the flow pattern. Others recent works concerning numerical simulations of laminar or turbulent flows in channels with porous insertions can be mentioned such as the work of Chan & Lien (2005) where it was examined the influence of permeability, forchheimer's constant and thickness on the flow (turbulent) in a planar channel which suffers a sudden expansion (backstep) with a porous insert. And, also, the work of de Lemos & Santos (2004) where it was analyzed the effect of porosity and permeability on the flow (laminar) and heat transfer in a channel with porous baffles.

The objective of this article is to analyze the porous insert influence on a turbulent flow in a pipe which suffers a sudden contraction (section area ratio of 0.285). The Reynolds number is 93,627 based on the pipe outlet diameter. The numerical tool to be used is the control volume technique in a generalized coordinate system. The macroscopic *k-ε* Low-Reynolds model is applied in all numerical calculations. First, the numerical result for a clear sudden contraction is compared with an experimental result available in the literature. Then, the same pipe is investigated with a porous insert placed just after the contraction. The new flow behavior is assessed by comparing the two cases, namely, with and without the porous insert. Attention is given to the pipe pressure losses and also for the flow patterns at the *vena contracta* region.

2. Geometry Under Consideration

Figure 1a presents the section, S_c, which is the effective section where the flow area is minimum. The area restriction is caused by the recirculation on the pipe wall just after the contraction. This phenomenon is called *vena contracta*, the minor loss increases even more (mainly during the expansion after the S_c section). Figure 1b shows a sketch of the porous insert in the pipe, the subscripts 1 and 2 represent the pipe inlet and outlet, respectively. In Figs. 1a and 1b, $\bar{u}_1$ and $\bar{u}_2$ are the mean velocities in a cross section on the axial direction, l_1 and l_2 are the pipe lengths, d_1 and d_2 or $2r_1$ and $2r_2$ are the diameters and a is the porous insert thickness. Two porous insert thickness are considered in this work, that are a/r_2 = 0.083 and a/r_2 = 0.166. The section pipe ratio is the same used in the work of Durst & Loy (1985), that is, S_2/S_1 = 0.285 or r_2/r_1 = 0.534.

a)

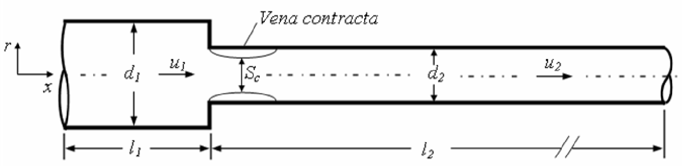

b)

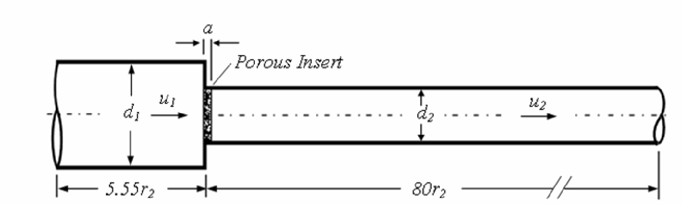

Figure 1. Simple sketch of the pipe geometry: (a) *vena contracta*; (b) porous insert.

3. Governing Equations

The governing equations used in this work have already been derived in details, Pedras & de Lemos (2001a-c) and for this reason their derivation need not to be repeated here. Essentially, the macroscopic form of the time-averaged governing equations is obtained by taking the volumetric mean of the entire equation set which is based on the concept of double decomposition, de Lemos & Pedras (2001), Pedras & de Lemos (2000). In this development, it is assumed a homogeneous, rigid porous medium saturated in an incompressible single-phase flow. Also, all physical properties are kept fixed.

The equations of the turbulent flow in porous media (neglecting the transient and gravitational terms) are given below.

The macroscopic continuity equation can be written as,

$$\nabla \cdot \bar{\mathbf{u}}_D = 0 \tag{1}$$

where $\bar{\mathbf{u}}_D$ is the average superficial velocity or Darcy velocity. The Eq.(1) was obtained by the application of the Dupuit-Forchheimer relationship, $\bar{\mathbf{u}}_D = \phi \langle \bar{\mathbf{u}} \rangle^i$, where ϕ is the porous medium porosity and $\langle \bar{\mathbf{u}} \rangle^i$ means the intrinsic (liquid) average of the local velocity vector $\bar{\mathbf{u}}$ (Gray & Lee (1977)).

The macroscopic momentum equation is given by,

$$\rho \nabla \cdot \left(\frac{\bar{\mathbf{u}}_D \bar{\mathbf{u}}_D}{\phi} \right) = -\nabla(\phi \langle \bar{p} \rangle^i) + \mu \nabla^2 \bar{\mathbf{u}}_D + \nabla \cdot (-\rho \phi \langle \overline{\mathbf{u}'\mathbf{u}'} \rangle^i) - \left[\frac{\mu \phi}{K} \bar{\mathbf{u}}_D + \frac{c_F \phi \rho |\bar{\mathbf{u}}_D| \bar{\mathbf{u}}_D}{\sqrt{K}} \right] \tag{2}$$

where the correlation $-\rho \overline{\mathbf{u}'\mathbf{u}'}$ is obtained after the application of the time-average operator to the local instantaneous momentum equation. Then, applying the volume-average procedure to the entire momentum equation (see Pedras & de Lemos (2001a) for details), results in the term $-\rho \phi \langle \overline{\mathbf{u}'\mathbf{u}'} \rangle^i$ of Eq.(2). This term is called here the Macroscopic Reynolds Stress Tensor (MRST). And, Eq. (2) is finally obtained by making use again of the relationship, $\bar{\mathbf{u}}_D = \phi \langle \bar{\mathbf{u}} \rangle^i$.

The last two terms in the right hand side of Eq.(2) represent the Darcy-Forchheimer contribution where the constant c_F is the Forchheimer coefficient. The term $\langle \overline{p} \rangle^i$ is the intrinsic average pressure of the fluid, ρ is the fluid density, μ represents the dynamic fluid viscosity and K is the porous medium permeability.

The term MRST, in Eq. (2), is modeled assuming the Boussinesq concept for clear fluid as follows,

$$-\rho\phi\langle \overline{\mathbf{u}'\mathbf{u}'} \rangle^i = \mu_{t_\phi} 2\langle \overline{\mathbf{D}} \rangle^v - \frac{2}{3}\phi\rho\langle k \rangle^i \mathbf{I} \tag{3}$$

where, $\mathbf{I}$ is the unity tensor, $\langle \overline{k} \rangle^i$ is the intrinsic average of the turbulent kinetic energy, and μ_{t_ϕ} is the macroscopic turbulent viscosity which is modeled similarly to the clear fluid. In Pedras & de Lemos (2001a), it was proposed a relationship for μ_{t_ϕ} as,

$$\mu_{t_\phi} = \rho c_\mu f_\mu \frac{\langle k \rangle^{i\,2}}{\langle \varepsilon \rangle^i} \tag{4}$$

where $\langle \overline{\varepsilon} \rangle^i$ is the intrinsic average of the dissipation rate of k and c_μ = 0.09. In Eq. (3) the term,

$$\langle \overline{\mathbf{D}} \rangle^v = \frac{1}{2}\left[\nabla(\phi\langle \overline{\mathbf{u}} \rangle^i) + \left[\nabla(\phi\langle \overline{\mathbf{u}} \rangle^i)\right]^T\right] \tag{5}$$

represents the mean macroscopic deformation tensor.

The macroscopic transport equations for $\langle \overline{k} \rangle^i = \langle \overline{\mathbf{u}'\mathbf{u}'} \rangle^i / 2$ and $\langle \overline{\varepsilon} \rangle^i = \mu\langle \overline{\nabla\mathbf{u}' : (\nabla\mathbf{u}')^T} \rangle^i / \rho$ in the k-ε High-Reynolds form were proposed in Pedras & de Lemos (2001a, and, also, adjusted for the k-ε Low-Reynolds (Pedras & de Lemos (2001c, 2003)) as follows,

$$\rho\nabla\cdot(\overline{\mathbf{u}}_D\langle k \rangle^i) = \nabla\cdot\left[(\mu + \frac{\mu_{t_\phi}}{\sigma_k})\nabla(\phi\langle k \rangle^i)\right] - \rho\langle \overline{\mathbf{u}'\mathbf{u}'} \rangle^i : \nabla\overline{\mathbf{u}}_D + c_k\rho\frac{\phi\langle k \rangle^i |\overline{\mathbf{u}}_D|}{\sqrt{K}} - \rho\phi\langle \varepsilon \rangle^i \tag{6}$$

$$\rho\nabla\cdot(\overline{\mathbf{u}}_D\langle \varepsilon \rangle^i) = \nabla\cdot\left[(\mu + \frac{\mu_{t_\phi}}{\sigma_\varepsilon})\nabla(\phi\langle \varepsilon \rangle^i)\right] + c_1\left(-\rho\langle \overline{\mathbf{u}'\mathbf{u}'} \rangle^i : \nabla\overline{\mathbf{u}}_D\right)\frac{\langle \varepsilon \rangle^i}{\langle k \rangle^i} + c_2 f_2 c_k\rho\frac{\phi\langle \varepsilon \rangle^i |\overline{\mathbf{u}}_D|}{\sqrt{K}} - c_2 f_2\rho\phi\frac{\langle \varepsilon \rangle^i}{\langle k \rangle^i} \tag{7}$$

where σ_k = 1.4, σ_ε = 1.3, c_1 = 1.5, c_2 = 1.9 are non-dimensional empirical constants, and, specially for the porous medium, c_k was found to be equal to 0.28 through numerical calculations by Pedras & de Lemos (2001a-c, 2003). Also, f_2 and f_μ are damping functions used in the k-ε Low-Reynolds model.

3.1. Boundary conditions

At the pipe inlet cross section, it is imposed a developed profile of velocity, k and ε (obtained numerically) and, at its outlet, a zero diffusion flux condition is set. On the walls, a non-slip condition is applied.

The Low-Reynolds model make use of two damping function, f_2 and f_μ, which are fully presented in Abe, Kondoh & Nagano (1994). In order to consider the viscous effects in the sublayer region, it is advisable that most first volumes should have n_p^+<1, where the subscript p refers to the first volume from the wall and the superscript + denotes a non-dimensional wall distance which is given by $n^+ = (u_\tau\, n/\nu)$. In the expression of the non-dimensional distance, $u_\tau = (\tau_w/\rho)^{1/2}$ is the friction velocity, τ_w is the shear stress of the first volume and ν is the kinematic viscosity.

4. Numerical Methods and Grid Independence

Equations (1), (2), (6) and (7) are discretized for a bi-dimensional axisymmetric domain, in generalized coordinates, involving both clean and porous media. In order to solve the discretized equations system, the control volume approach is employed and, the SIMPLE algorithm is used for handling the velocity-pressure coupling, Patankar (1980). The Flux

Blended Deferred squeme is used for the interpolation functions of the convective flux, more details in Khosla & Rubin (1974). Concerning the numerical method implemented, see Pedras & de Lemos (2001b) for more details.

Concerning the numerical calculations, at each iteration the residues of the momentum equations at the axial and radial coordinates are calculated and also of the k, ε and mass conservation equation. Thus, as a convergence criterion, a maximum normalized residue was set to 10^{-6}.

In order to verify the grid independence of the results, three meshes were used in the case of a sudden contraction without porous insert. The results of k_c (contraction minor loss coefficient, which will be explained in the following section) were 0.420, 0.424 and 0.425 for 31,626, 68,652 and 116,457 control volumes, respectively. A difference of approximately 0.2% in the values of k_c between the two greater grids was low enough to consider the results grid-independent in terms of clear flow. In the literature, there are no experimental results available with porous insert, this way, it was not possible to evaluate the grid independence for such cases. Therefore, the mesh of size 220 x 102 (upstream the pipe contraction) and 924 x 52 (downstream the pipe contraction) is used in all numerical calculations. A partial view of the computational domain (at the *vena contracta* region) is presented in Fig. 2. It is clearly observed a concentration of grid points towards the wall and the *vena contracta* region. In all calculations, the Low-Reynolds model condition of $n_p^+<1$ was satisfied.

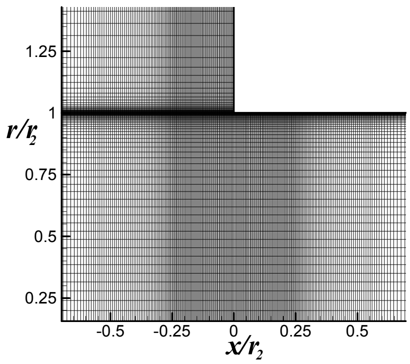

Figure 2. Partial view of the computational grid at the *vena contracta* region.

5. Results and Discussion

5.1. Clear flow

The geometry considered is of a pipe which suffers a sudden contraction. The section area contraction ratio (S_2/S_1) is 0.285. All geometric parameters are non-dimensional based on the outlet pipe radius, r_2. In order to have a negligible influence of the inlet and outlet pipe section in the results, the inlet and outlet pipe length were found to be, l_1/r_2 = 5.55 and l_2/r_2 = 80, respectively. Also, it was verified that the length, downstream the contraction, of l_2/r_2 = 80 is long enough to consider the flow fully developed in its outlet cross section, condition necessary to use Eq. 14 and to assure the validity of a zero diffusion flux as a boundary condition at the pipe outlet.

In all results presented in this work, it was considered an outlet Reynolds number of 93,627 based on the pipe outlet diameter (d_2) and an inlet Reynolds number of 50,000 based on the pipe inlet diameter (d_1).

Considering the pipe with sudden contraction, a numerical simulation without the porous insert was carried out and the minor loss obtained from the calculations was compared with an experimental result available in the literature, Streeter (1961). The minor loss due to the contraction (h_c) can be defined as:

$$h_c = k_c \frac{(\overline{u}_2)^2}{2} \tag{8}$$

where, k_c is the contraction minor loss coefficient (non-dimensional value). This value does not account for the major losses but only for the minor loss due to the contraction. In Streeter (1961), experimental values of k_c without porous insert are presented for several geometries on turbulent flows. The k_c is not significantly affected with the Reynolds number in fully turbulent flows. Thus, according to Streeter (1961), for an outlet Reynolds number of 93,627 and $S_2 / S_1 = 0.285$, the k_c value is found to be 0.367 (see Streeter (1961), pp. 3-21, Tab. 3.2).

Considering the energy conservation between two cross sections of steady incompressible flow and under the assumption of no external work and uniform internal energy and pressure across the two sections results, Fox & McDonald (1998),

$$h_T = \left(\frac{p_1}{\rho} + \alpha_1 \frac{(\overline{u}_1)^2}{2} + g z_1 \right) - \left(\frac{p_2}{\rho} + \alpha_2 \frac{(\overline{u}_2)^2}{2} + g z_2 \right) \tag{9}$$

where h_T is the total head loss between the two sections, p is the pressure in each section, g is the acceleration of gravity, α is the kinetic energy coefficient and z is the coordinate which corresponds to the height level of the pipe section. Subscriptions 1 and 2 refer to the inlet and outlet cross section area, respectively. The kinetic energy coefficient, α, is defined as,

$$\alpha = \frac{\int_S \rho u^3 dS}{\dot{m}\, \overline{u}^2} \tag{10}$$

where $\dot{m}$ is the mass flow rate in the pipe.

The major losses, h_l, can be written as a function of the friction factor, f_a,

$$h_l = f_a \frac{l}{d} \frac{\overline{u}^2}{2} \tag{11}$$

The total head loss is the sum of all major and minor losses, and considering the case of a pipe with a sudden contraction, h_T is given by,

$$h_T = h_l + h_c = f_{a1} \frac{l_1}{d_1} \frac{(\overline{u}_1)^2}{2} + f_{a2} \frac{l_2}{d_2} \frac{(\overline{u}_2)^2}{2} + k_c \frac{(\overline{u}_2)^2}{2} \tag{12}$$

where f_{a1} and f_{a2} are the friction factor due to the major losses upstream and downstream the pipe contraction, respectively.

We can define the pressure coefficient, Cp, as,

$$Cp = \frac{p - p_b}{\rho (u_2)^2 / 2} \tag{13}$$

where, p_b is a reference pressure which is, here, assumed to be nul, and, p is a local pressure.

Substituting Eq. (12), (13) in Eq. (9), and assuming that the inlet and outlet cross section have fully developed flow and same height level coordinate, the minor loss coefficient can be obtained as,

$$k_c = Cp_1 - Cp_2 - \alpha_2 + \left[\alpha_1 \left(\frac{\overline{u}_1}{\overline{u}_2} \right)^2 - \frac{f_{a1}}{2} \frac{l_1}{r_2} \frac{r_2}{r_1} \left(\frac{\overline{u}_1}{\overline{u}_2} \right)^2 - \frac{f_{a2}}{2} \frac{l_2}{r_2} \right] \tag{14}$$

where the last three terms (between square brackets) depend only on the pipe geometry, the Reynolds number and the pipe wall roughness which is always considered smooth. Therefore, it does not change in the cases, here, studied. Therefore, the k_c value will only depend on the pressure coefficient difference between the pipe inlet and outlet cross secion (Cp_1 - Cp_2) and on α_2.

In Eq. 14, the values of α_1 = 1.089 and f_{a1} = 0.02297 were obtained through a numerical simulation, using Re = 50,000, in a pipe with only the pipe inlet diameter (d_1), where a periodic condition between its inlet and outlet was applied. Also, using the same periodic conditions but with the outlet diameter (d_2) and Re = 93,627 the value of f_{a2}

was found to be 0.01936. Also, through the numerical calculation of the pipe with a contraction, the value of $Cp_1 - Cp_2$ were found to be 2.187.

Substituting all geometrical and obtained numerical parameters in Eq. 14, the k_c was found to be 0.424, which means a percent deviation of 15.7 % in comparison with the experimental value (k_c = 0.367) of Streeter (1961). This deviation can be expected since in Assato & de Lemos (2000), where a *k*-*ε* Low-Reynolds turbulence model was employed in a backstep geometry, the deviation from the experimental value of the reattachment length was of 22.86 %.

5.2. Porous insert

The *vena contracta* is the main responsible for the minor loss after the contraction. Therefore, one of the objectives of the porous insert is to eliminate or reduce the *vena contracta*, although the porous insert itself increases the losses. This way, there is a compromise between the losses caused by the porous insert and the gain in eliminating or diminishing the *vena contracta*. In the results, even that all cases present losses higher than the case of clear flow, the flow behavior is analyzed in order to evaluate it for such cases.

In this section, the numerical results of a sudden contraction pipe with a porous insertion are presented. Concerning the porous insert, it was used two different thicknesses (a/r_2 = 0.083 and a/r_2 = 0.166), three values of permeability represented by the Darcy Number (Da = 8.56x10^{-3}, Da = 8.56x10^{-5}, Da = 8.56x10^{-7}) and it was used a porosity (ϕ) of 0.85, making 6 different types of porous insertions. The Darcy number is a non-dimensional parameter related to the permeability (K) by the following expression,

$$Da = \frac{K}{(d_2)^2} \tag{15}$$

The values of k_c for each porous insert with the three different values of Da are presented in Tab. 1. It is noted a large increase of k_c with lower Da in comparison with the k_c value without porous insert of 0.424.

Table 1. k_c numerical values for each porous insert (ϕ = 0.85)

k_c			
a/r_2	Da		
	8.56x10^{-3}	8.56x10^{-5}	8.56x10^{-7}
0.083	0.991	5.41	49.42
0.166	1.480	10.37	99.87

The streamlines at the *vena contracta* region are presented in Figs. 3a-d and 4a-d, the rectangles represent the porous insert regions. It is noted that as the Da value decreases, the vortex size is significantly damped and it is completely suppressed for Da = 8.56x10^{-7}. Also, it is noticed that the recirculation size diminishes slightly for the thicker porous insert considering the same Da.

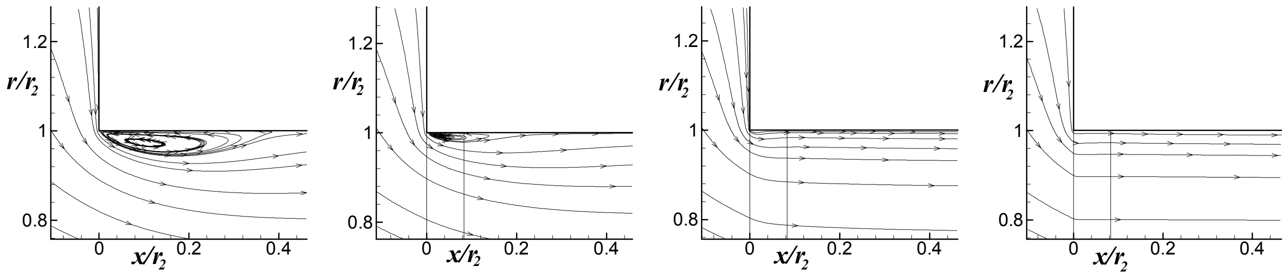

(a) (b) (c) (d)

Figure 3. Comparison of streamlines (ϕ = 0.85): (a) a/r_2 = 0; (b) a/r_2 = 0.083 and $Da = 8.56x10^{-3}$; (c) a/r_2 = 0.083 and $Da = 8.56x10^{-5}$; (d) a/r_2 = 0.083 and $Da = 8.56x10^{-7}$

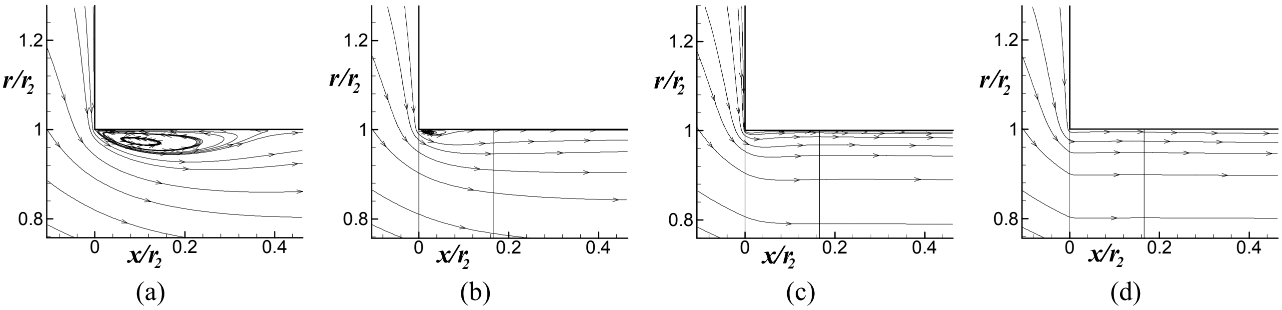

Figure 4. Comparison of streamlines (ϕ = 0.85): (a) a/ r_2 = 0; (b) a/ r_2 = 0.166 and $Da = 8.56x10^{-3}$; (c) $a/r_2 = 0.166$ and $Da = 8.56x10^{-5}$; (d) a/ r_2 = 0.166 and $Da = 8.56x10^{-7}$

Figure 5 presents the values of the friction coefficient (C_f) along the pipe outlet wall of the cases with and without porous insert. The friction coefficient is defined as follows,

$$C_f = \frac{\tau_w}{\rho(\bar{u}_2)^2/2} \tag{16}$$

In Fig. 5a-b, the negative values of C_f indicate the existence of a recirculation. The recirculation is completely suppressed by the porous insert for Da = 8.56x10^{-7} since no negative values of C_f are observed in Fig 5a-b for such cases which is in accordance with Figs. 3d and 4d. Also, it is noted that the C_f values are much more affected by the Da numbers than the porous thicknesses used. For Da = 8.56x10^{-5} and Da = 8.56x10^{-7}, it is clearly observed that the C_f values keeps much higher values inside the porous insert indicating that most of the pressure loss occurs inside it.

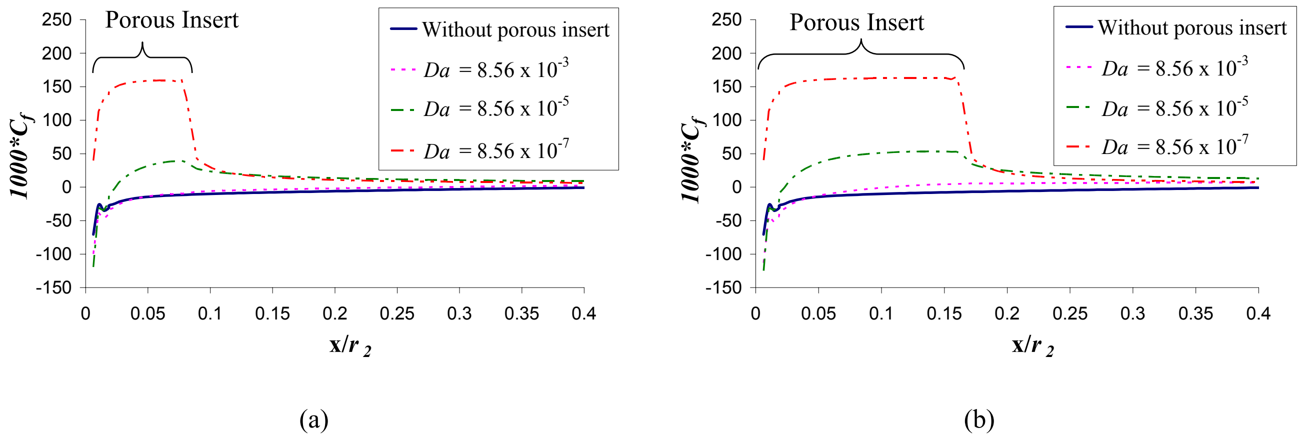

Figure 5. Comparison of C_f values on the pipe outlet wall without and with porous insert (ϕ = 0.85): (a) a/ r_2 = 0.083; (b) a/ r_2 = 0.166

6. Conclusion

Although the recirculation size (at the *vena contracta* region) was reduced due to the porous insert, the minor loss was always higher than the case without porous insert. Therefore, according to the numerical results, we can conclude that the losses caused by the porous insert itself are more significant than the gain due to the reduction of the *vena contracta*. Anyway, it was presented the influence of the permeability and thickness on the losses and on the vortex size which can be useful when a specific flow pattern is needed, for example, in order to control the heat exchange as stated in Assato & de Lemos (2004a-d).

Another fact is that the k_c numerical value without the porous insert was approximately 15.7% higher than the experimental result. For future works, the authors intend to analyze the pipe by employing a non-linear turbulent model since in Assato et. al. (2005) better results were obtained with the use of such model.

7. Acknowledgements

The authors are thankful to FAPESP and CNPq, Brazil, for their financial support during the course of this research.

8. References

Abe, K, Kondoh, T. & Nagano, Y, 1994, "A new turbulence model for predicting fluid fluid flow and heat transfer in separating and reattaching flows-1. Flow field calculations", Int. J. Heat Mass Transfer, vol.37, pp. 139-151.

Assato, M. & de Lemos, M.J.S., 2000, "Tratamento numérico e aplicações de um modelo de viscosidade turbulenta não linear para alto e baixo reynolds"(in portuguese), Escola Brasileira de Primavera Transição e Turbulência, Uberlândia, Brazil, 11-15 Dec.

Assato, M. & de Lemos, M.J.S, 2002, "Heat transfer in a suddenly expanded turbulent flow past a porous insert using linear and non-linear eddy-viscosity models", ASME Int. Mechanical Eng. Congress and Exposition, New Orleans, Lousiana, USA, November.

Assato, M. & de Lemos, M.J.S., 2003, "Heat transfer in a back-step flow past a porous insert using a Non-Linear Turbulence model and a Low Reynolds wall treatment", 3rd Int. Conf. on Computational Heat and Mass Transfer, Univ. of Calgary, Banff, Canada.

Assato, M. & de Lemos, M.J.S., 2004a, "Simulation of heat transfer in a forward-facing step flow with a porous insert using linear and non-linear k-ε models", Int. Conf. on Porous Media and Applications, Évora, Portugal, 24-27 May.

Assato, M. & de Lemos, M.J.S., 2004b, "Estudo da transferência de calor turbulenta em uma contração abrupta com inserto poroso usando modelos de turbulência linear e não linear" (in Portuguese), Proc. 10th Brazilian Cong. of Thermal Sciences and Engineering, Rio de Janeiro, Brazil, Nov. 29-Dec. 03.

Assato, M. & de Lemos, M.J.S., 2004c, "Turbulent heat transfer in an abrupt contraction channel with a porous obstacle using a non-linear model with a high Reynolds number wall function", III Cong. National de Eng. Mecânica, Belém, Brazil, 10-13 August.

Assato, M. & de Lemos, M.J.S., 2004d, "Flow and heat transfer past a sudden contraction with a porous insert using linear and non-linear turbulence models", ASME Int. Mechanical Eng. Congress and Exposition, Anaheim, CA, USA, November.

Assato, M., Pedras, M.H.J. & de Lemos, M.J.S., 2005, "Numerical solution of turbulent flow past a backward-facing-step with a porous insert using linear and non-linear k-ε models", J.Porous Media, vol. 8, no.1, pp.13-29.

Astarita, G. & Greco, G., 1968, "Excess pressure drop in laminar flow through sudden contraction. I & EC Fundamentals", vol. 7, no. 1, pp. 27-31.

Chan, C.C. & Lien, F-S, 2005, "Permeability effects of turbulent flow through a porous insert in a backward-facing-step channel", Transport in Porous Media, vol 59, no. 1, pp. 47-71.

de Lemos, M.J.S. & Pedras, M.H.J., 2001, "Recent mathematical models for turbulent flow in saturated rigid porous media", J. Fluids Eng., vol. 123, pp. 935-940.

de Lemos, M.J.S., Santos, N.B., 2004, "Laminar heat transfer in a parallel plate channel with solid and porous baffles", Proc. of IMECE04, 2004 ASME Int. Mechanical Eng. Congress, Nov. 13-20, Anahein, CA.

Durst, F. & Loy, T., 1985, "Investigations of laminar flow in a pipe with sudden contraction of cross sectional area", Comp. & Fluids, vol. 13, no. 1, pp. 15-36.

Fox, R. W. & McDonald, A. T., 1998, "Introduction to Fluid Mechanics", 5th ed., John Wiley & Sons, New York.

Gray, W.G., Lee, P.C.Y., 1977, "On the theorems for local volume averaging of multiphase system", Int. J. Multiphase Flow, vol.12, pp.401-410.

Khosla, P.K. & Rubin, S.G., 1974, "A diagonally dominant second-order accurate implicit scheme", Comp. & Fluids, vol. 2, pp. 207.

Patankar, S.V., 1980, "Numerical heat transfer and fluid flow", Mc-Graw Hill.

Pedras, M.H.J. & de Lemos, M.J.S., 2000, "On the definition of turbulent kinetic energy for flow in porous media", Int. Commun. Heat and Mass Transfer, vol. 27, no. 2, pp. 211-220.

Pedras, M.H.J. & de Lemos, M.J.S., 2001a, "Macroscopic turbulence modeling for incompressible flow through undeformable porous media", Int. J. Heat Mass Transfer, vol. 44, n. 6, pp. 1081-1093.

Pedras, M.H.J. & de Lemos, M.J.S., 2001b, "Simulation of turbulent flow in porous media using a spatially periodic array and a Low Re Two-Equation closure", Numerical Heat Transfer - Part A Appl., vol. 39, no. 1, pp. 35-59.

Pedras, M.H.J. & de Lemos, M.J.S., 2001c, "On the mathematical description and simulation of turbulent flow in a porous media formed by an array of elleptic rods", J. Fluids Eng., vol.123, no.4, pp.941-947.

Pedras, M.H.J. & de Lemos, M.J.S., 2003, "Computational of turbulent flow in porous media using a Low-Reynolds k-ε model and an infinite array of transversally displaced elliptic rods", Numerical Heat Transfer - Part A Appl., vol. 43, no. 1, pp. 585-602.

Streeter, V.L., 1961, ed. Handbook of Fluid Dynamics. McGraw-Hill, New York.